

Causal Analysis of the Quantum States

Sergey M. Korotaev and Evgeniy O. Kiktenko

*Geoelectromagnetic Research Centre of Schmidt Institute of Physics of the Earth, Russian Academy of Sciences,
P.O. 30 Troitsk, Moscow Region 142190, Russia*

Abstract. We suggest quantum generalization of the method of causal analysis used before only for the classical variables. The causality parameters for the series of examples of two-qubit entangled states are computed. The results are compared with the concurrence and degree of mixedness of the states. The role of state asymmetry in quantum information transfer is shown. For the qubits under nonuniformity external magnetic field the nontrivial role of this nonuniformity for subsystem causal connection has been studied. At last quantum causal analysis helps to understand Cramer principle of weak causality which admits extraction of information from the future without the classical paradoxes.

Keywords: causality, entanglement, information, time

PACS: 03.65.Ud, 03.67.Mn

I. INTRODUCTION

In spite of the fact, that principle of causality is widely used in physics, it does not mean more than retardation of the effect relative to the cause. However the retardation is necessary but not sufficient condition of the causal connection (“Post hoc non est propter hoc”). But what is a cause and what is an effect remains formally indefinite. Meanwhile in the simple situations we usually well realize what is a cause and what is an effect, not measuring a retardation, but only implicating it (e.g. without any measurement of the retardation, it is obvious causal-effect relation of the current in the lamp and photocell circuits). In the complicated situations, in the systems with feedbacks, usual intuitive understanding of causality may lead to the confusions, and hence the desirability of its formalization is obvious. The fact that in the simple situation location of the causes and effects is clear without retardation measuring indicates that these conceptions are asymmetrical in themselves. The problem is to define this asymmetry formally and not invoking the time relation, which has to be introduced *after* the definition as an axiom. From the solution of this problem originally directed to formalization of Kozyrev’s causal mechanics [1], the method of causal analysis was born [2], turned out to be useful in various classical applications (e.g. [3-17]). It was found fruitful in the construction of the models of complicated systems with feedbacks by experimental data, as well as in the estimation of the influence of noise-forming impacts in the real open systems.

This work is devoted to development of analogous approach to quantum mechanics, where solving of the similar problems seems no less burning. This is especially true in regard to quantum nonlocality, which since its discovery has been attracting attention above of all by unusualness of quantum correlations from the viewpoint of principle of causality. It is assumed that quantum correlations realize instantaneously, but since for the communication purposes one has to use an ancillary classical channel, the violation of causality becomes experimentally unverifiable. The implementation of causal analysis has to give the possibility to investigate this situation by the strict and universal way. At last the implementation of causal analysis is burning for solving of the concrete questions of quantum information (the most neatly formulated in [18]) concerning peculiarities of behavior of the asymmetrical entangled states.

In Sec. II the short review of the kernel of classical causal analysis formalism is presented. In Sec. III the extension of causal analysis to the quantum variables is considered. In Sec. IV application of causal analysis is demonstrated to the symmetrical states, where causality is absent, but nevertheless the quantitative characteristics of the mixed states can be obtained. Sec. V is dedicated to the analysis of asymmetrical mixed states examples of increasing complexity, beginning with the illustrative obtaining of causality measure and ending with the nontrivial conclusions about causal connection nature depending on the external magnetic field and temperature. The general results are summarized in Sec. VI.

II CLASSICAL CAUSAL ANALYSIS

Consider the classical variables A and B describing the respective subsystems of the bipartite system AB , their Shannon marginal and conditional entropies:

$$\begin{aligned} S(A) &= -\sum_{j=1}^J P(A_j) \log_2 P(A_j), \\ S(B) &= -\sum_{k=1}^K P(B_k) \log_2 P(B_k), \end{aligned} \quad (1)$$

$$\begin{aligned} S(A|B) &= -\sum_{k=1}^K P(B_k) \sum_{j=1}^J P(A_j|B_k) \log_2 P(A_j|B_k), \\ S(B|A) &= -\sum_{j=1}^J P(A_j) \sum_{k=1}^K P(B_k|A_j) \log_2 P(B_k|A_j), \end{aligned} \quad (2)$$

where $P(A_j)$, $P(B_k)$ are the probabilities of j -th (k -th) levels of A and B respectively; $P(A_j|B_k)$, $P(B_k|A_j)$ are the respective conditional probabilities. Define the following parameters: the marginal α and conditional β asymmetries:

$$\alpha = \frac{S(B)}{S(A)}, \quad 0 \leq \alpha \leq \infty; \quad \beta = \frac{S(B|A)}{S(A|B)}, \quad 0 \leq \beta \leq \infty; \quad (3)$$

and the independence functions:

$$i_{B|A} = \frac{S(B|A)}{S(B)}, \quad i_{A|B} = \frac{S(A|B)}{S(A)}, \quad 0 \leq i \leq 1. \quad (4)$$

Meaning of the independence functions is enough transparent: at $i_{B|A} = 1$, B is independent of A , at $i_{B|A} = 0$, B is one-valued function of A . In other words, the values $1-i$ determine the unilateral dependences of the variables. The direct and inversed independences must coincide only in the limiting case: $i_{B|A} = 1 \Leftrightarrow i_{A|B} = 1$.

Next introduce the causality function γ :

$$\gamma = \frac{i_{B|A}}{i_{A|B}}, \quad 0 \leq \gamma \leq \infty \quad (5)$$

The name is derived from the particular values of γ . $\gamma = 0$: B is the one-valued function of A , but not the reverse. It is possible to interpret that as the utmost irreversible process $A \Rightarrow B$. $\gamma = 1$: A and B to the same extent depend on one another, that is naturally to identify with absence of causality. $\gamma = \infty$: A is one-valued function of B , but not the reverse. It is possible to interpret that as the utmost irreversible process $B \Rightarrow A$.

Consider the space of parameters α , β , $i_{B|A}$ ($\gamma = \beta/\alpha$ is equivalent to (5)) displayed in Fig.1. In this space it is possible to obtain the classification of any type of dependence of B on A . Every type is imaged by a point. Analyzing the limiting cases and using the reversibility of information:

$$I = S(B) - S(B|A) = S(A) - S(A|B), \quad (6)$$

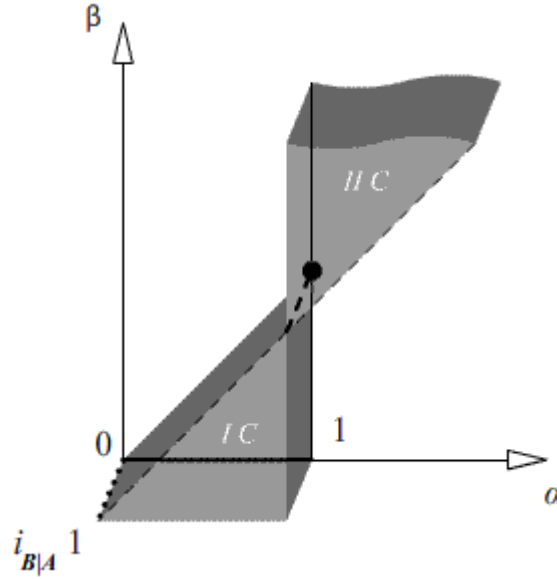


FIGURE 1. Classical entropic diagram (IC is normal causality, IIC is inversed causality, dotted line is the B -constant line, thick solid line is the one-valued function line, fine dashed line is the independence line, thick dashed line is the adiabat, circle is the mutually one-valued function point).

it is easily to prove, that the forbidden regions are: (i) the subspace $\alpha < 1, \gamma \geq 1$; (ii) the subspace $\alpha > 1, \gamma \leq 1$; (iii) the plane $\beta = 1$ except the line of intersection with the plane $\alpha = 1$; (iv) the plane $\alpha = 1$ except the line of intersection with the plane $\beta = 1$ and except the line of intersection with the plane $i_{B|A} = 0$; (v) the plane $\beta = 0$ except the axis segment $\alpha \in [0, 1]$ and axis $i_{B|A}$; (vi) the plane $\alpha = 0$ except the axis $i_{B|A}$; (vii) the plane $i_{B|A} = 0$ except the line $\alpha = 1$ and axis segment $\alpha \in [0, 1]$; (viii) the plane $i_{B|A} = 1$; except the line $\gamma = 1$; (ix) the plane $\gamma = 1$, except the axis $i_{B|A}$, line $i_{B|A} = 1$ and line $\alpha = \beta = 1$.

In the allowed space it is possible to separate out, on parameter meaning grounds, the following regions:

- Subspace of normal causality: $\gamma < 1, \beta < 1, \alpha < 1$.
- Subspace of inversed causality: $\gamma > 1, \beta > 1, \alpha > 1$.
- B -constant line: $B = const$ independently of A .
- One-valued function line: $i_{B|A} = 0, \beta = 0, 0 < \alpha < 1$. Here $S(B|A) = 0$, i.e. B is fully determined by A , but not reverse.
- Independence line: $i_{B|A} = 1, \gamma = 1$.
- Mutually one-valued function point: $(i_{B|A} = 0, \alpha = \beta = 1)$. Here $S(B|A) = S(A|B) = 0$.
- Adiat: $\alpha = \beta = 1$, that corresponds to the isentropic process.

It is sufficiently for the formal definition of classical causality.

Definition 1. The cause A and the effect B are variables for which $\gamma < 1$.

Analyzing meaning of γ it is not difficult to see that our definition includes usual intuitive understanding of causality (at least with an eye physicist's intuition). Indeed, if we say that A is the cause and B is the effect, we keep in mind fully or partly determined dependence of B on A , such that inversed dependence is absent. Our definition allows refining: the inversed dependence is less than direct one and how much. The causeless functional and statistical dependences are also known. We neatly fix this class: $\gamma = 1$. If, having studied statistics of the arbitrary denoted variables A and B , we find $\gamma > 1$, it simply means that B is the cause and A is the effect. Besides full formality, our definition has an obvious advantage of the quantitative measure over common used the qualitative one. On theoretical and multiplicity of experimental examples of the classical problems (e.g. [3-12]) it had been shown that such formal definition of causality did not contradict its intuitive understanding in the simple situations and could be used in the complicated ones.

Our definition allows formulation of the axiom of classical causality as follows:

$$\gamma < 1 \Rightarrow \tau > 0, \gamma > 1 \Rightarrow \tau < 0, \gamma \rightarrow 1 \Rightarrow \tau \rightarrow 0, \quad (7)$$

where τ is time shift of B relative to A .

Note, that $\gamma < 1 \Rightarrow \alpha < 1$, $\gamma > 1 \Rightarrow \alpha > 1$, (the reversed is wrong, that is why α can not be used for the definition of causality). This necessary condition is a manifestation of 7-th Shannon theorem [19] on decrease of the entropies from a channel input $A(B)$ to its output $B(A)$.

Consider an elementary cause-effect link from information exchange standpoint. According to the theorem about noisy channel capacity, the upper limit of information reception rate in B from A is:

$$\sup v_{A \rightarrow B} = \frac{1}{\delta t} \frac{S(B) - S(B|A)}{S(B)}, \quad (8)$$

where δt is duration of an elementary signal, the numerator is maximized by variation of the A distributions. Replacing the rate (8) by the lower limit of time and using (4), we have:

$$\inf t_{A \rightarrow B} = \frac{\delta t}{1 - i_{B|A}} \quad (9)$$

In a like manner for the reversed transfer:

$$\inf t_{B \rightarrow A} = \frac{\delta t}{1 - i_{A|B}} \quad (10)$$

By the condition $\gamma < 1 \Leftrightarrow 1 - i_{B|A} > 1 - i_{A|B} \Leftrightarrow t_{A \rightarrow B} < t_{B \rightarrow A}$. The finite difference of times (10) and (9) means that in any time lapse the effect obtains from the cause more information than the cause does from the effect. Information excess in the effect means the irreversibility of information flow. Than time of information excess reception Δt is:

$$\Delta t = \delta t \left(\frac{1}{1 - i_{A|B}} - \frac{1}{1 - i_{B|A}} \right) \quad (11)$$

Supposing that the subsystem A and B are separated by some finite effective distance Δr , one can determine the linear velocity of irreversible information flow $c_2 = \Delta r / \Delta t$ (the notation follows the tradition of Ref. [1], where originally, although in less rigorous terms, the course of time pseudoscalar c_2 of the same meaning was introduced):

$$c_2 = k \frac{(1 - i_{A|B})(1 - i_{B|A})}{i_{A|B} - i_{B|A}} = k \frac{(1 - i_{B|A} / \gamma)(1 - i_{B|A})}{i_{B|A}(1 / \gamma - 1)} \quad (12)$$

where $k = \Delta r / \delta t$. It is easy to see that the sign of c_2 is mutually one-valued related with the value of γ relative to 1:

$$\gamma < 1 \Leftrightarrow c_2 > 0, \gamma > 1 \Leftrightarrow c_2 < 0, \gamma \rightarrow 1 \Leftrightarrow c_2 \rightarrow \pm\infty, \quad (13)$$

therefore it is possible to replace γ by c_2 in the causality definition and axiom.

The causal analysis apparatus has been generalized to the causal network in the multipartite system [7]. The influence of the different kinds of noise-forming impacts from the non-controlled environment on all the parameters $(\alpha, \beta, i_{B|A}, i_{A|B}, \gamma)$, the possibilities of other classical entropy definitions different from Shannon one as well as the

foliated spaces of the probability definition have been analyzed [12]. The method has been tested on the problems of classical electrodynamics [3-6] and on data of various classical experiments (e.g. [4-12]).

III QUANTUM QAUSAL ANALYSIS

For the quantum variables von Neumann entropy is used. We have instead of Eqs. (1) and (2):

$$S(A) = -\text{Tr}\rho_A \log_2 \rho_A, S(B) = -\text{Tr}\rho_B \log_2 \rho_B, \quad (14)$$

$$S(B|A) = S(AB) - S(A), S(A|B) = S(AB) - S(B), \quad (15)$$

where $\rho_A = \text{Tr}_B \rho_{AB}$, $\rho_B = \text{Tr}_A \rho_{AB}$, $S(AB) = -\text{Tr}\rho_{AB} \log_2 \rho_{AB}$. Note, that although the conditional entropies can be in principle directly calculated through the conditional entropies by analogy with Eqs. (2) [20], practically it is simple to calculate them indirectly according to Eqs. (15).

For the entangled states the conditional entropies can be negative [20, 21]. Therefore $-\infty \leq \beta \leq \infty$, $-1 \leq i \leq 1$, $-\infty \leq \gamma \leq \infty$. In particular, for the bipartite states from Schmidt decomposition it is follows $\alpha = 1$, $\beta = 1$, $\gamma = 1$, $i_{B|A} = i_{A|B} = -1$. The entropic diagram is extended (Fig. 2). Besides the two classical subspaces C the four quantum ones Q are allowed:

- I C $0 \leq \alpha \leq 1, 0 \leq \beta \leq 1, 0 \leq i_{B|A} \leq 1, 0 \leq \gamma \leq 1, c_2 > 0;$
- II C $1 \leq \alpha \leq \infty, 1 \leq \beta \leq \infty, 0 \leq i_{B|A} \leq 1, 1 \leq \gamma \leq \infty, c_2 < 0;$
- IQ $0 \leq \alpha \leq 1, 1 \leq \beta \leq \infty, -1 \leq i_{B|A} \leq 0, 1 \leq \gamma \leq \infty, c_2 > 0;$
- IIQ $1 \leq \alpha \leq \infty, 0 \leq \beta \leq 1, -1 \leq i_{B|A} \leq 0, 0 \leq \gamma \leq 1, c_2 < 0;$
- IIIQ $0 \leq \alpha \leq 1, -\infty \leq \beta \leq 0, -1 \leq i_{B|A} \leq 0, -\infty \leq \gamma \leq 0, c_2 > 0;$
- IVQ $1 \leq \alpha \leq \infty, -\infty \leq \beta \leq 0, 0 \leq i_{B|A} \leq 1, -\infty \leq \gamma \leq 0, c_2 < 0.$

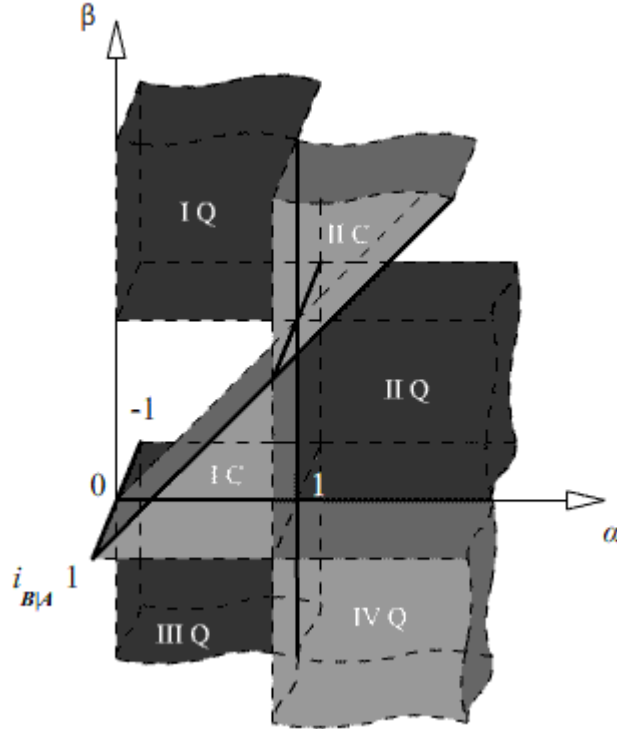


FIGURE 2. Quantum entropic diagram.

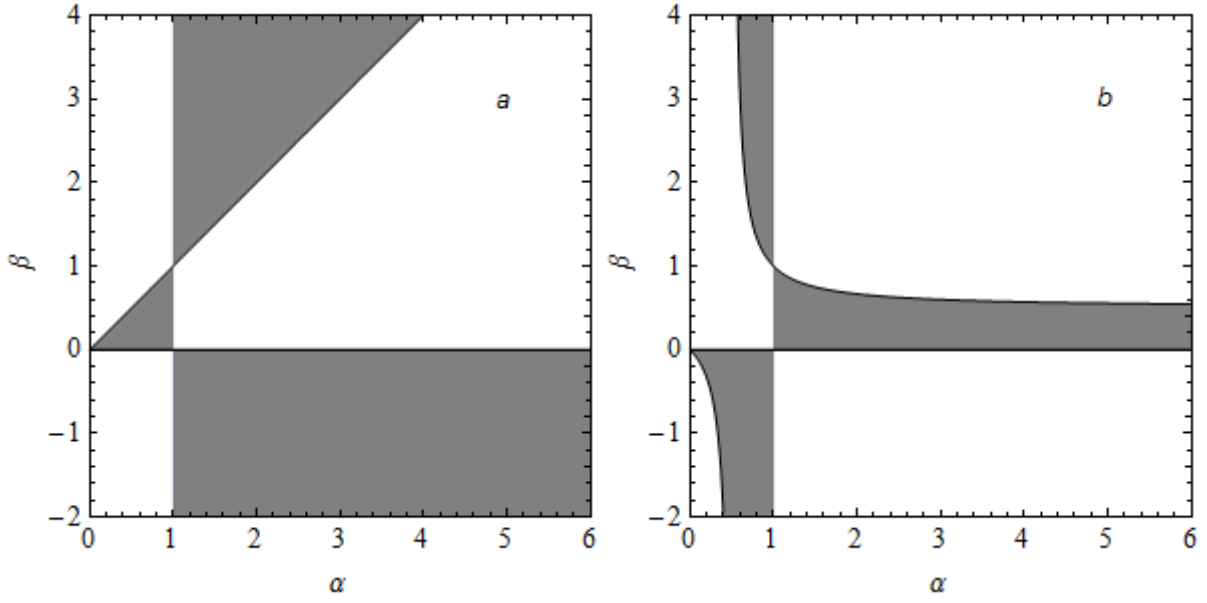


FIGURE 3. The allowed subspaces in the sections $i_{B|A} = \text{const}$: (a) the subspaces IC, IIC and IVQ; (b) the subspaces IQ, IIQ and IIIQ.

However in the 3D diagram of Fig.2 it is difficult to show the demarcation of the allowed subspaces. For their indication invoke the fact that the independence function $i_{B|A}$ can be represented as follows:

$$i_{B|A} = \frac{\beta(\alpha - 1)}{\alpha(\beta - 1)} \quad (16)$$

In the subspaces IC, IIC and IVQ $0 \leq i_{B|A} \leq 1$, that according to Eq. (16), brings to the system of two inequalities with respect to α, β . Their solutions in the form of sections $i_{B|A} = \text{const}$ are presented in Fig.3a. The allowed subspaces are adjacent to the border planes. In the subspaces IQ, IIQ and IVQ $-1 \leq i_{B|A} \leq 0$. The solutions of corresponding couple of the inequalities are presented in Fig. 3b. The allowed subspaces are separated from the part of border planes by the hyperbolic surfaces.

At the quantum level the value of γ is insufficient for distinguishing the cause and effect. But by reference to correspondence between c_2 and γ in both the classical subspaces and necessary condition of the 7-th Shannon theorem obeying in all the six subspaces: $c_2 > 0 \Rightarrow \alpha < 1$, $c_2 < 0 \Rightarrow \alpha > 1$ it is possible to give the definition of causality appropriate for the quantum variables.

Definition 2: *The cause A and the effect B are the states for which $c_2 > 0$.*

Then, introducing the demand of the effect retardation τ , we can formulate the axiom of strong causality, embracing local and nonlocal correlations, as follows:

$$c_2 > 0 \Rightarrow \tau > 0, c_2 < 0 \Rightarrow \tau < 0, |c_2| \rightarrow \infty \Rightarrow \tau \rightarrow 0. \quad (17)$$

Notice, that nonlocal correlations are often treated as instantaneous and causeless ones. Our approach includes such treatment, but only as a particular case.

The axiom (17) is the principle namely of strong causality. Cramer was the first to distinguish the principles of strong and weak causality [22]. The strong causality corresponds to the usual condition of retardation of the effect relative to the cause. Without this axiom we have the weak causality. The weak causality corresponds only to non-local correlations and implies a possibility of information transmission in reverse time, but only related with unknown states (hence “the telegraph to the past” is impossible).

Eqs. (8) – (12) remain true by virtue of the parallelism of classical and quantum information theory [21]. A justified in Ref. [23] interpretation of entanglement of a quantum system as the resource serving for information transfer through it, gives them the additional physical meaning. Specifically in Ref. [23] it has been proven that negative conditional entropy is “an amount of information which can be transmitted through < the subsystems > 1 and 2 from a system interacting with 1 to another system interacting with 2. The transmission medium is quantum entanglement between 1 and 2.” Causality characterized by c_2 value reflects the asymmetry of this process (the greater causality is expressed the less $|c_2|$).

But though defined by Eq. (12) c_2 with accuracy to the coefficient k is of great interest by itself, it is desirable to show the way of its full determination for the natural processes. For this there is no remain δt to be duration of “an elementary signal”, that is pertinent only for a technical channel. Since δt in any case plays a role of some elementary time it is natural to suppose it, according to Ref. [24] to be time of brachistochrone evolution. In the case of time independent Hamiltonian this time is easily expressed explicitly:

$$\delta t = \frac{\hbar \theta}{2\omega} \quad (18)$$

where 2ω is the difference between the largest and smallest eigenvalues of the Hamiltonian and θ is the length of geodesic (according to Fabini-Study metric) connecting the initial and final states. If they are orthogonal, $\theta = \pi$. In realistic Hamiltonian ω depends on distance Δr and k becomes definite. It is readily shown [2] that for the simplest Coulomb interaction $k = e^2 / \hbar$, that corresponds to Kozyrev order estimation of c_2 obtained from the semiclassical reasoning.

To keep the examples described bellow from becoming too involved; we shall restrict ourselves by calculations of c_2 with accuracy to $k = 1$. Only in the last example we shall demonstrate the more precise estimation with regard to δt , which variable dependent on eigenvalues of Hamiltonian (remaining $\Delta r = 1$).

IV. SYMMETRIC STATES

By the symmetric two-partite states are meant the states with equal subsystem entropies: $S(A) = S(B)$, $\alpha = \beta = \gamma = 1$, $|c_2| \rightarrow \infty$. The causality is absent (adiabatic state connection). However the value $i_{B|A} = i_{A|B}$ is finite and can be related to the mixedness measures $\text{Tr} \rho_{AB}^2$ or $S(AB)$ and to the standard entanglement measure-concurrence C [25]:

$$C = \max(\sqrt{\lambda_1} - \sqrt{\lambda_2} - \sqrt{\lambda_3} - \sqrt{\lambda_4}, 0) \quad (19)$$

where λ_i are eigenvalues of the matrix $\rho \tilde{\rho}$. Spin-flip matrix $\tilde{\rho}$ is defined as:

$$\tilde{\rho} = (\sigma_y \otimes \sigma_y) \rho^* (\sigma_y \otimes \sigma_y) \quad (20)$$

We show below that employment of causal analysis make sense, naturally, only for the mixed states. At the beginning we consider the elementary systems, when mixedness emerges as a result of extraction of the two subsystems from a three-partite pure state, thereupon – more containable situations, when the mixedness is a result of interaction with a non-controlled environment. Since such interaction leads to decoherence, analysis of these situation we shall begin with the basic mechanisms of decoherence – depolarization and dephasing (dissipation, which may lead to the asymmetry is considered in Sec. V.A). Next we consider typical mixed states in their initial and asymptotic species (after long-run dissipation).

A. Pure States

The entropic symmetry is evident from Schmidt decomposition. Consider the arbitrary pure states:

$$|\Phi\rangle = \alpha|00\rangle + \beta|11\rangle, \quad (21)$$

or

$$|\Psi\rangle = \alpha|01\rangle + \beta|10\rangle, \quad (22)$$

where $|\alpha|^2 + |\beta|^2 = 1$. Since the state is pure $\text{Tr}\rho_{AB}^2 = 1$, $S(AB) = 0$, concurrence C varies according to ratio of α and β . But at any nonzero α and β the independence function is constant: $i_{B|A} = -1$. Therefore for the pure states the causal analysis is of no interest.

B. GHZ State

It is known, that GHZ state

$$|\Psi\rangle = \frac{1}{\sqrt{2}}(|000\rangle + |111\rangle) \quad (23)$$

is marked by that in spite of the maximal entanglement of three particles (ABC), the pairwise entanglement is absent: $C = 0$. The two-partite state is mixed: $\text{Tr}\rho_{AB}^2 = \frac{1}{2}$, $S(AB) = 1$. Therewith $i_{B|A} = 0$. The entanglement is absent but the particles A and B are maximally classically correlated.

C. W-State

$$|W\rangle = \frac{1}{\sqrt{3}}(|001\rangle + |010\rangle + |100\rangle) \quad (24)$$

Similar to GHZ state, W-state is entangled three-partite state, but the pairwise concurrence $C = \frac{2}{3}$ (moreover, (24) and in general N -partite W-state represents the case of arranged in pairs and equal entanglement of the all N particles [26]). The mixedness of the two-partite subsystem is somewhat weaker than for GHZ: $\text{Tr}\rho_{AB}^2 = \frac{5}{9}$, $S(AB) = -\frac{1}{3}\log_2 \frac{1}{3} - \frac{2}{3}\log_2 \frac{2}{3} \approx 0.918$. However, likewith GHZ state: $i_{B|A} = 0$.

D. Depolarization

Depolarization reduces to the following transformation [27, 28]:

$$\begin{aligned} |0\rangle\langle 0| &\rightarrow (1-p)|0\rangle\langle 0| + p\frac{I}{2}, \\ |1\rangle\langle 1| &\rightarrow (1-p)|1\rangle\langle 1| + p\frac{I}{2}, \\ |1\rangle\langle 0| &\rightarrow (1-p)|1\rangle\langle 0|, \\ |0\rangle\langle 1| &\rightarrow (1-p)|0\rangle\langle 1|, \end{aligned} \quad (25)$$

where $0 \leq p \leq 1$ is decoherence degree. Take the singlet for the initial state:

$$|\Psi^-\rangle = \frac{1}{\sqrt{2}}(|01\rangle - |10\rangle), \quad (26)$$

and let us assume that only the second particle (B) is depolarized. The depolarized density is:

$$\begin{aligned} \rho_{AB} = & \frac{1}{2} \left(\frac{p}{2} |00\rangle\langle 00| + (1-\frac{p}{2}) |01\rangle\langle 01| + \frac{p}{2} |11\rangle\langle 11| + \right. \\ & \left. (1-\frac{p}{2}) |10\rangle\langle 10| - (1-p) |01\rangle\langle 10| - (1-p) |10\rangle\langle 01| \right) \end{aligned} \quad (27)$$

In spite of the fact that only one particle is depolarized, both the reduced densities are equal to each other, i.e. the system is symmetric:

$$\rho_A = \rho_B = \frac{1}{2} (|0\rangle\langle 0| + |1\rangle\langle 1|). \quad (28)$$

On finding the eigenvalues, we obtain:

$$S(AB) = -\frac{3p}{4} \log_2 \frac{p}{4} - (1-\frac{3p}{4}) \log_2 (1-\frac{3p}{4}), \quad (29)$$

$$S(A) = S(B) = 1. \quad (30)$$

The independence function is:

$$i_{B|A} = S(AB) - 1. \quad (31)$$

The concurrence is:

$$C = \max(1 - \frac{3p}{2}, 0). \quad (32)$$

The dependence of $i_{B|A}$, C , $Tr\rho_{AB}^2$ on p is shown in Fig.4. It is seen that $i_{B|A}$ varies with decoherence degree in the full range from -1 at $p=0$ to $+1$ at $p=1$ (full depolarization), when correlation of the subsystems fully disappears. The independence increases according to the increase of mixedness in both its measures (exactly proportional for $S(AB)$) and to the decrease of concurrence. It is the most interesting that there is an interval $\frac{1}{4} < p < \frac{2}{3}$, where $i_{B|A} > 0$ and $C > 0$. On this interval the system is in an entropic sense is classical but nevertheless entangled.

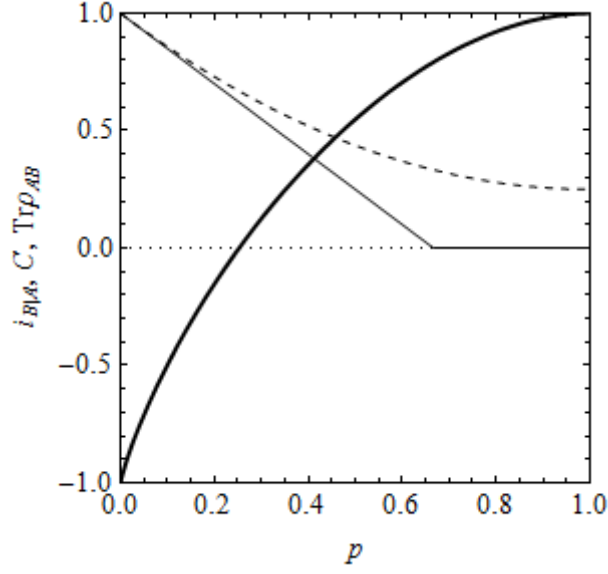


FIGURE 4. Dependence of $i_{B|A}$ (thick solid line), C (fine solid line), and $\text{Tr}\rho_{AB}^2$ (dashed line) on degree of depolarization p of the state (26).

E. Dephasing

The transformation is [27,28]:

$$\begin{aligned} |1\rangle\langle 0| &\rightarrow (1-p)|1\rangle\langle 0|, \\ |0\rangle\langle 1| &\rightarrow (1-p)|0\rangle\langle 1|. \end{aligned} \quad (33)$$

The state (26) after dephasing of the particle B is:

$$\rho_{AB} = \frac{1}{2}(|01\rangle\langle 01| - (1-p)|01\rangle\langle 10| - (1-p)|10\rangle\langle 01| + |10\rangle\langle 10|). \quad (34)$$

Eqs. (28), (30) and (31) are true again, but

$$S(AB) = -(1-\frac{p}{2})\log_2(1-\frac{p}{2}) - \frac{p}{2}\log_2\frac{p}{2}, \quad (35)$$

$$C = 1 - p. \quad (36)$$

Therefore by full dephasing $i_{B|A} = 0$, i.e. the subsystems remain classically maximally correlated. By partial dephasing C and negative $i_{B|A}$ are the characteristics of entanglement on equal terms (Fig.5).

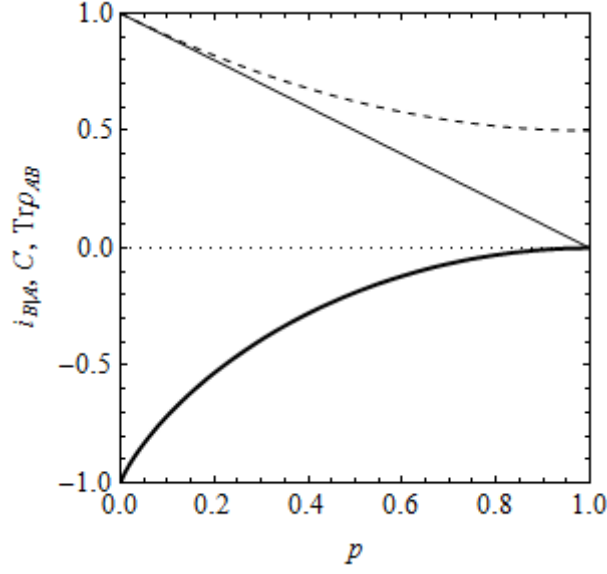


FIGURE 5. Dependence of $i_{B|A}$ (thick solid line), C (fine solid line) and $\text{Tr}\rho_{AB}^2$ (dashed line) on degree of dephasing p of the state (26).

F. Bell-Diagonal States

Initial Bell-diagonal states are:

$$\rho_{AB} = p_1 |\Phi^+ \rangle\langle\Phi^+| + p_2 |\Phi^- \rangle\langle\Phi^-| + p_3 |\Psi^+ \rangle\langle\Psi^+| + p_4 |\Psi^- \rangle\langle\Psi^-| \quad (37)$$

where

$$|\Phi^\pm \rangle = \frac{1}{\sqrt{2}}(|00\rangle \pm |11\rangle), \quad |\Psi^\pm \rangle = \frac{1}{\sqrt{2}}(|10\rangle \pm |01\rangle) \quad (38)$$

Eqs. (28), (30) and (31) are true again, but

$$S(AB) = -\sum_{i=1}^4 p_i \log_2 p_i \quad (39)$$

$$C = \max(2 \max\{p_i\} - 1, 0) \quad (40)$$

Behavior of $i_{B|A}$, C and $\text{Tr}\rho_{AB}^2$ in deciding on $p_4 = p$, $p_1 = p_2 = p_3 = (1-p)/3$ is shown in Fig. 6. It is seen that $i_{B|A}$ reflects the mixedness achieving 1 at equality of the all p_i . But more important, that there is an interval $0.5 < p < 0.81$, where $i_{B|A} > 0$ and $C > 0$. On this interval the system is entangled in spite of the entropic classicness.

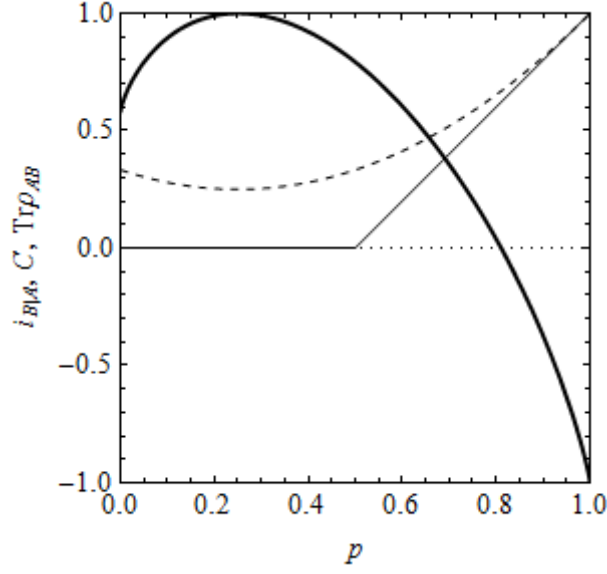


FIGURE 6. Dependence of $i_{B|A}$ (thick solid line), C (fine solid line) and $\text{Tr}\rho_{AB}^2$ (dashed line) on $p = p_4$ of initial Bell-diagonal states (37).

Now consider dissipation of the states (37) at the presence of a common bath. It is known that against before accepted views, dissipation may not reduce to decoherence, but on the contrary, may play a constructive role in entanglement generation [29-36]. Following Ref. [34], suppose that the qubits represent the two-level atoms separated by a distance small compared to the radiation wavelength. Dissipation occurs at the expense of spontaneous emission of the photons, which have a substantial probability to be absorbed by the other atom. In Ref. [34] the system dynamic equation is solved and the asymptotic solutions $t \rightarrow \infty$ are analyzed in detail. In particular the asymptotic density matrix at the initial one (37) is:

$$\rho_{AB}^{as} = \begin{pmatrix} 0 & 0 & 0 & 0 \\ 0 & \frac{p_4}{2} & -\frac{p_4}{2} & 0 \\ 0 & -\frac{p_4}{2} & \frac{p_4}{2} & 0 \\ 0 & 0 & 0 & 1-p_4 \end{pmatrix} \quad (41)$$

Hence

$$S(AB) = -p_4 \log_2 p_4 - (1-p_4) \log_2 (1-p_4) \quad (42)$$

$$S(A) = S(B) = -\frac{p_4}{2} \log_2 \frac{p_4}{2} - (1-\frac{p_4}{2}) \log_2 (1-\frac{p_4}{2}) \quad (43)$$

$$i_{B|A} = \frac{S(AB)}{S(A)} - 1 \quad (44)$$

$$C = p_4 \quad (45)$$

The constructive role of dissipation is that even the initial state was separable ($C = 0$) the asymptotic one is entangled in the all range of finite p_4 . Figure 7 demonstrates that in this case the independence function does not reflect

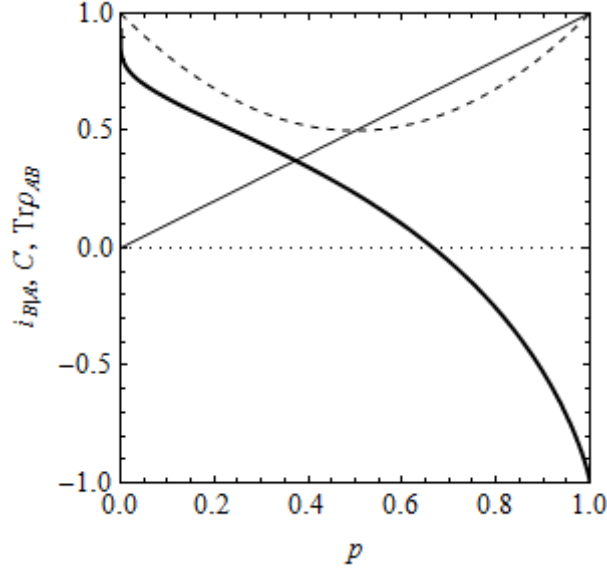


FIGURE 7. Dependence of $i_{B|A}$ (thick solid line), C (fine solid line) and $\text{Tr}\rho_{AB}^2$ (dashed line) on $p = p_4$ of asymptotic Bell-diagonal states (41).

the mixedness, but does reflect the concurrence. Therewith $i_{B|A} \leq 1$, i.e. the system is correlated at almost any p_4 ($\max i_{B|A} = 1$ is achieved at $p_4 = 0$). On the interval $0 \leq p_4 < 0.67$ $i_{B|A} > 0$ (classical) at rather strong entanglement.

G. Werner States

The initial Werner states

$$\rho_{AB} = p \frac{I}{4} + (p-1) |\Phi^+ \rangle \langle \Phi^+| \quad (46)$$

represent a depolarized triplet, for which as well as for the singlet, the expressions (28) – (32) and Fig. 4 are true.

Consider the result of described in above subsection dissipation process of the states (46). According to Ref. [34] in the asymptotic limit $t \rightarrow \infty$:

$$\rho_{AB}^{ss} = \begin{pmatrix} 0 & 0 & 0 & 0 \\ 0 & \frac{p}{8} & -\frac{p}{8} & 0 \\ 0 & -\frac{p}{8} & \frac{p}{8} & 0 \\ 0 & 0 & 0 & 1 - \frac{p}{4} \end{pmatrix} \quad (47)$$

Hence:

$$S(AB) = -\frac{p}{4} \log_2 \frac{p}{4} - (1 - \frac{p}{4}) \log_2 (1 - \frac{p}{4}) \quad (48)$$

$$S(A) = S(B) = -\frac{p}{8} \log_2 \frac{p}{8} - (1 - \frac{p}{8}) \log_2 (1 - \frac{p}{8}) \quad (49)$$

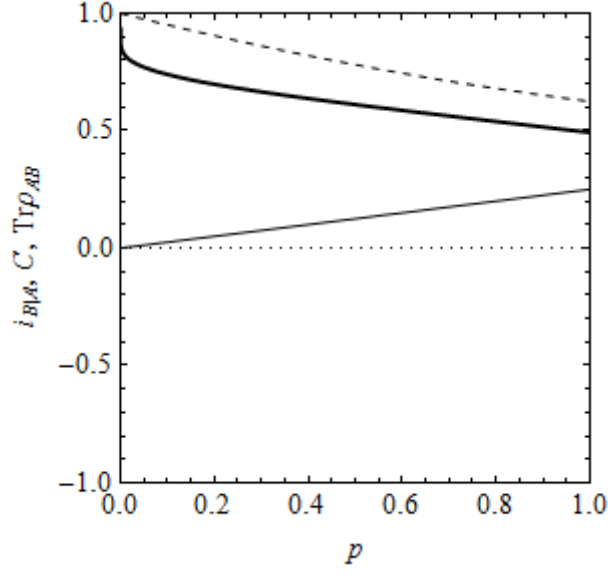


FIGURE 8. Dependence of $i_{B|A}$ (thick solid line), C (fine solid line) and $\text{Tr}\rho_{AB}^2$ (dashed line) on $p = p_4$ of asymptotic Werner states (47).

$$C = \frac{p}{4} \quad (50)$$

Figure 8 shows that asymptotic Werner states radically differ from the initial ones: They are not only entangled at any $p > 0$, but the concurrence increases with the increase of p – the smaller entangled initial state the greater entangled dissipated one. Therewith $i_{B|A}$ is positive (classical) at any p ($\max i_{B|A} = 1$ at $p = 0$, $\min i_{B|A} \approx 0.493$ at $p = 1$). It is remarkable that the decrease of $i_{B|A}$ and the increase of C are practically proportional to the increase of mixedness.

H. Maximally Entangled Mixed States

In Ref. [37] it is conjectured that at fixed $\text{Tr}\rho_{AB}^2$ the maximally entangled are the states:

$$\rho_{AB} = \begin{pmatrix} h(\delta) & 0 & 0 & \frac{\delta}{2} \\ 0 & 1-2h(\delta) & 0 & 0 \\ 0 & 0 & 0 & 0 \\ \frac{\delta}{2} & 0 & 0 & h(\delta) \end{pmatrix}; h(\delta) = \begin{cases} \frac{1}{3}, & \delta \in \left[0, \frac{2}{3}\right] \\ \frac{\delta}{2}, & \delta \in \left[\frac{2}{3}, 1\right] \end{cases} \quad (51)$$

Hence:

$$S(AB) = -(1-2h)\log_2(1-2h) - \left(h - \frac{\delta}{2}\right)\log_2\left(h - \frac{\delta}{2}\right) - \left(h + \frac{\delta}{2}\right)\log_2\left(h + \frac{\delta}{2}\right) \quad (52)$$

$$S(A) = S(B) = -h\log_2 h - (1-h)\log_2(1-h) \quad (53)$$

$i_{B|A}$ is determined by Eq. (44), the concurrence is

$$C = \delta \quad (54)$$

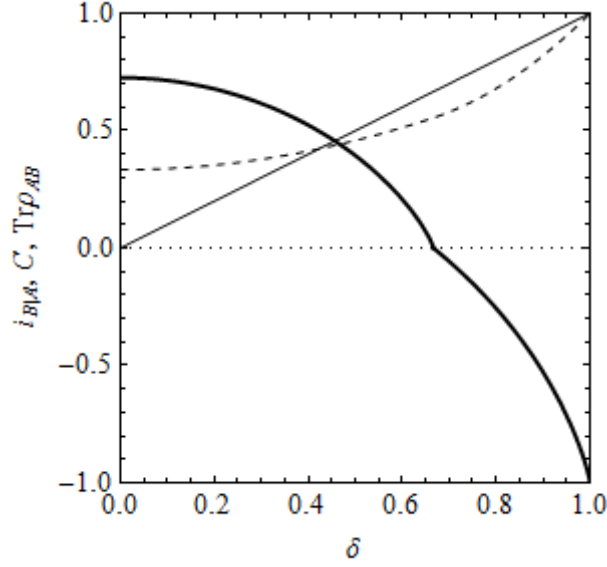


FIGURE 9. Dependence of $i_{B|A}$ (thick solid line), C (fine solid line) and $\text{Tr}\rho_{AB}^2$ (dashed line) on δ of initial maximally entangled mixed states (51).

The dependence of $i_{B|A}$, C , $\text{Tr}\rho_{AB}^2$ on δ is shown in Fig. 9. $i_{B|A}$ changes from $+0.725$ at $\delta=0$ to -1 , at $\delta=1$ and its decrease as whole reflects the decrease of mixedness. Therewith on the interval $0 < \delta < \frac{2}{3}$ $i_{BA} > 0$ at $C > 0$ – the states are entangled in spite of the entropic classiness.

According to solution of Ref. [34], the asymptotic result of dissipation of the state (51) is:

$$\rho_{AB}^{as} = \begin{pmatrix} 0 & 0 & 0 & 0 \\ 0 & \frac{1}{4}(1-2h) & -\frac{1}{4}(1-2h) & 0 \\ 0 & -\frac{1}{4}(1-2h) & \frac{1}{4}(1-2h) & 0 \\ 0 & 0 & 0 & \frac{1}{2}+h \end{pmatrix} \quad (55)$$

Hence:

$$S(AB) = -\left(\frac{1}{2}+h\right)\log_2\left(\frac{1}{2}+h\right) - \left(\frac{1}{2}-h\right)\log_2\left(\frac{1}{2}-h\right) \quad (56)$$

$$S(A) = S(B) = -\left(\frac{1}{4}-\frac{h}{2}\right)\log_2\left(\frac{1}{4}-\frac{h}{2}\right) - \left(\frac{3}{4}+\frac{h}{2}\right)\log_2\left(\frac{3}{4}+\frac{h}{2}\right) \quad (57)$$

$i_{B|A}$ is determined by Eq. (44), the concurrence is:

$$C = \frac{1}{2}(1-2h) \quad (58)$$

Figure 10 shows that dissipated maximally entangled mixed states are characterized by radically different dependence of C on δ , hence at small δ they are more entangled than the initial ones. As this take place, as a result of dissipation the system has become in entropic terms classical ($0.571 \leq i_{B|A} \leq 1$ at all δ). In contrast to the initial

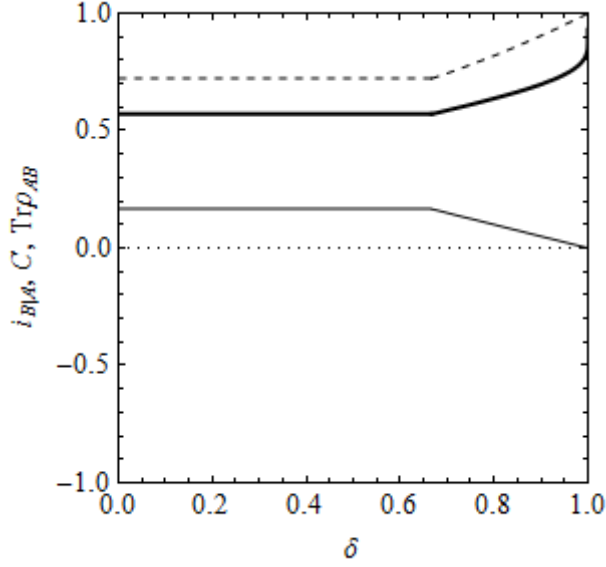


FIGURE 10. Dependence of $i_{B|A}$ (thick solid line), C (fine solid line) and $\text{Tr}\rho_{AB}^2$ (dashed line) on δ of asymptotic maximally entangled mixed states (55).

states the independence function varies inversely to the degree of mixedness. In the pure state limit $\delta \rightarrow 0$: $S(AB) \rightarrow 0$, $\text{Tr}\rho_{AB}^2 \rightarrow 1$, but also $S(A) = S(B) \rightarrow 0$, therefore $i_{B|A} = i_{A|B} \rightarrow 1$.

Qualitatively asymptotic maximally entangled mixed states are close to asymptotic Werner states by the relation of independence, concurrence and mixedness.

V. ASYMMETRIC STATES

In this section we consider the examples of asymmetric states, for which application of causal analysis is the most substanceble. The examples are considered in ascending order of nontriviality. In the computations of c_2 we shall suppose $k=1$ until the last example, where we shall consider the variable k . Note, that in those examples we shall nowhere use the axiom of strong causality (17). Reverse time is allowed.

A. Asymmetric Dissipation

Consider the third possible way of decoherence that is dissipation by the same manner as in. Sec. IV. D and E: only one particle B is dissipated. Therein lies dissimilarity from the symmetric dissipation considered in Sec. IV. E – H.

The dissipation reduces to the following transformation [27, 28]:

$$\begin{aligned}
 |0\rangle\langle 0| &\rightarrow |0\rangle\langle 0|, \\
 |1\rangle\langle 1| &\rightarrow (1-p)|1\rangle\langle 1| + p|0\rangle\langle 0|, \\
 |1\rangle\langle 0| &\rightarrow \sqrt{1-p}|1\rangle\langle 0|, \\
 |0\rangle\langle 1| &\rightarrow \sqrt{1-p}|0\rangle\langle 1|.
 \end{aligned} \tag{59}$$

The singlet (26) is taken as the initial state as well as in Sec. IV. D and E. The dissipated density is:

$$\begin{aligned}
 \rho_{AB} = \frac{1}{2} [&p|00\rangle\langle 00| + (1-p)|01\rangle\langle 01| - \sqrt{1-p}|01\rangle\langle 10| - \\
 &\sqrt{1-p}|10\rangle\langle 01| + |10\rangle\langle 10|].
 \end{aligned} \tag{60}$$

The reduced densities are:

$$\rho_A = \frac{1}{2}(|0\rangle\langle 0| + |1\rangle\langle 1|), \quad (61)$$

$$\rho_B = \frac{1}{2} (1+p)|0\rangle\langle 0| + (1-p)|1\rangle\langle 1|. \quad (62)$$

The entropies are:

$$S(AB) = -\frac{p}{2} \log_2 \frac{p}{2} - (1-\frac{p}{2}) \log_2 (1-\frac{p}{2}), \quad (63)$$

$$S(A) = 1. \quad (64)$$

$$S(B) = -\frac{1+p}{2} \log_2 \frac{1+p}{2} - \frac{1-p}{2} \log_2 \frac{1-p}{2}. \quad (65)$$

The independence functions are:

$$i_{B|A} = \frac{S(AB)-1}{S(B)}; i_{A|B} = S(AB) - S(B). \quad (66)$$

The concurrence is:

$$C = \sqrt{1-p}. \quad (67)$$

From Fig. 11 it is clear that dissipation differs from depolarization and dephasing by more values of C in the all p range, while $i_{B|A}$ is negative everywhere similar to the dephasing case. But the main interest represents Fig. 12, where the measures of causality c_2 and γ are presented. $c_2 > 0$, therefore the particle A is the cause and B is the effect. It is in full agreement with the intuitive expectation – the irreversible flow of information is directed to the dissipating particle B . The decrease of c_2 with the increase of p also responds to intuitive expectation of amplification of causal connection with the increase of dissipation. But employment of the classical measure γ would lead at $0 < p < \frac{1}{2}$ to the opposite conclusion about directionality of the causal connection, while at $\frac{1}{2} < p < 1$ γ becomes classically meaningless.

In the entropic diagram (Fig. 2) the states (60) correspond to subspaces IQ (at $0 \leq p \leq \frac{1}{2}$) and IIIQ (at $\frac{1}{2} \leq p \leq 1$). The transition between the subspaces does not break smoothness of $c_2(p)$.

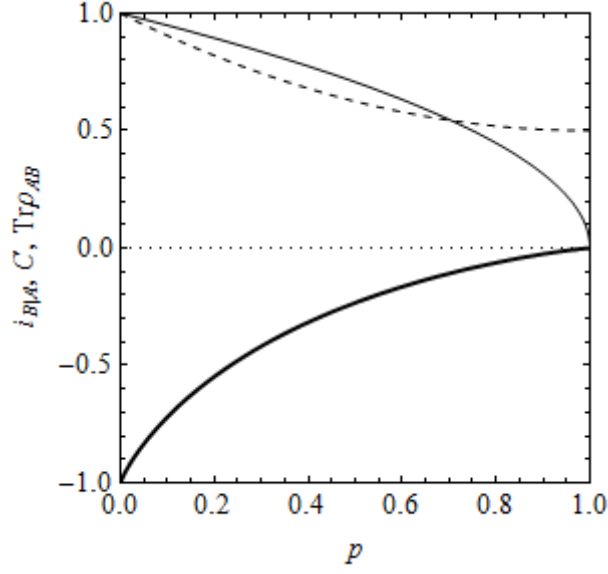


FIGURE 11. Dependence of $i_{B|A}$ (thick solid line), C (fine solid line), and $\text{Tr}\rho_{AB}^2$ (dashed line) on degree of dissipation p of the state (26).

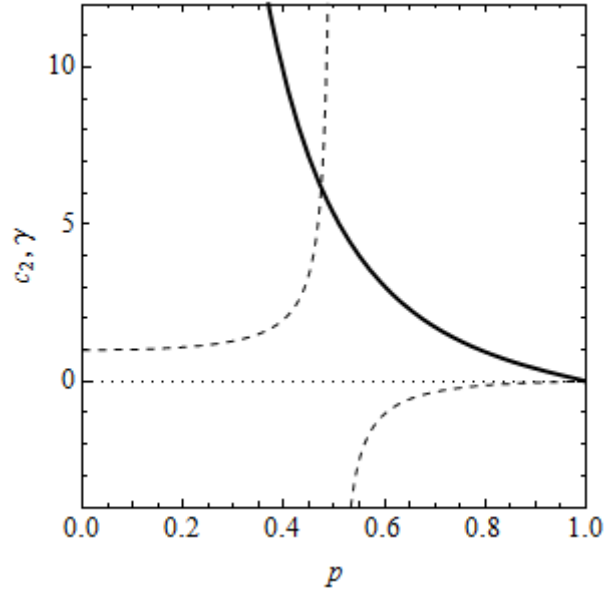


FIGURE 12. Dependence of c_2 (solid line) and γ (dashed line) on degree of dissipation p of the state (26).

B. One Particle is Entangled with Two Others.

Consider the case when one particle A is entangled equally and maximally with two others B and C . It is the three-partite state [26]:

$$|\Psi\rangle = \frac{1}{\sqrt{2}}|100\rangle + \frac{1}{2}(|001\rangle + |010\rangle). \quad (68)$$

Take the pair AB . The reduced densities are:

$$\rho_{AB} = \frac{1}{4}|00\rangle\langle 00| + \frac{1}{2}|10\rangle\langle 10| + \frac{1}{2\sqrt{2}}|10\rangle\langle 01| + \frac{1}{2\sqrt{2}}|01\rangle\langle 10| + \frac{1}{4}|01\rangle\langle 01|, \quad (69)$$

$$\rho_A = \frac{1}{2}(|0\rangle\langle 0| + |1\rangle\langle 1|), \quad (70)$$

$$\rho_B = \frac{3}{4}|0\rangle\langle 0| + \frac{1}{4}|1\rangle\langle 1|. \quad (71)$$

The entropies are:

$$S(AB) = S(B) = -\frac{3}{4}\log_2 \frac{3}{4} - \frac{1}{4}\log_2 \frac{1}{4} \approx 0.811, \quad (72)$$

$$S(A) = 1. \quad (73)$$

The independences are:

$$i_{B|A} \approx -0.233; i_{A|B} = 0. \quad (74)$$

The measures of causality are:

$$\gamma = -\infty; c_2 \approx 5.299. \quad (75)$$

The concurrence is:

$$C = \frac{1}{\sqrt{2}}. \quad (76)$$

According to the quantum measure c_2 A is the cause and B is the effect, while the classical measure γ is meaningless (the subspace IIIQ in the entropic diagram). In the pair AC the result is the same and thus A is the common cause for B and C . Classical intuition in this case would be powerless to distinguish the common cause from the common effect.

Intuition gives only true, by virtue of the symmetry, answer about the absence of causal connection of B and C . The similar mathematics for this couple give: $i_{B|C} = i_{C|B} \approx 0.233$, $\gamma = 1$, $|c_2| = \infty$, $C = \frac{1}{2}$. The particles B and C are entangled and classically correlated due to availability of the common cause. Note that the mixedness, according to both the measures in the pairs AB (AC) is less than in the pair BC : $S(AB) \approx 0.811$, $\text{Tr}\rho_{AB}^2 \approx 0.625$, $S(BC) = 1$, $\text{Tr}\rho_{AB}^2 = \frac{1}{2}$.

C. WRr-State

In Refs. [38,39] the different three-partite states related by the symmetry transformations, the particular cases of which are GHZ and W-states, have been investigated.

In particular the duplet has been obtained:

$$|WRr\rangle = \frac{1}{\sqrt{6}}(|001\rangle + |010\rangle - 2|100\rangle). \quad (77)$$

This state differs by the entanglement distribution from W-state considered in Sec. IV.C, for which $C_{AB} = C_{AC} = C_{BC} = \frac{1}{3}$, and the state considered in Sec. V.B, for which $C_{AB} = C_{AC} = \frac{1}{\sqrt{2}}$, $C_{BC} = \frac{1}{2}$. For the state (77)

$C_{AB} = C_{AC} = \frac{2}{3}$, $C_{BC} = \frac{1}{3}$ [38,39], that is the pair BC has entanglement twice smaller than two another pairs have.

For the state (77):

$$\rho_{AB} = \frac{1}{6}(4|10\rangle\langle 10| - 2|10\rangle\langle 01| - 2|01\rangle\langle 10| + |01\rangle\langle 01| + |00\rangle\langle 00|), \quad (78)$$

$$S(AB) = S(B) = -\frac{1}{6}\log_2 \frac{1}{6} - \frac{5}{6}\log_2 \frac{5}{6} \approx 0.651, \quad (79)$$

$$S(A) = -\frac{1}{3}\log_2 \frac{1}{3} - \frac{2}{3}\log_2 \frac{2}{3} \approx 0.918, \quad (80)$$

$$i_{B|A} \approx -0.412; i_{A|B} = 0, \quad (81)$$

$$\gamma = -\infty; c_2 \approx 3.43. \quad (82)$$

The same is true for the pair AC . Therewith $\text{Tr}\rho_{AB}^2 = \text{Tr}\rho_{AC}^2 \approx 0.722$.

As in Sec. V.B A is the cause for B and C and only the quantum measure of causality has a meaning (the subspace IIIQ in Fig. 2). The quantitative difference implies that according to both the measures of mixedness in the causal links of the state (77) it is less than in (68), and though the concurrence is less, the independence functions $i_{B|A} = i_{C|A} < 0$ are lower, i.e. quantum correlations are stronger, and c_2 is lower, i.e. causal connection is expressed stronger.

For the particles B and C in the state (77) we have: $S(BC) \approx 0.918$, $\text{Tr}\rho_{BC}^2 \approx 0.556$, $i_{B|C} = i_{C|B} \approx 0.412$, $\gamma = 1$, $|c_2| = \infty$, $C = \frac{1}{3}$. As with the state (68), causality in the pair BC is absent, and although the mixedness is lower, but the entanglement and classical ($i_{B|C} = i_{C|B} > 0$) correlations are weaker.

D. Asymmetric “Quantum-Classical” States

The question on the peculiarities of behavior of the asymmetric states was the first to set in Ref. [18], where the case of “quantum-classical” two-partite states was considered. The subsystem A is called quantum if $S(A) > S(AB)$, and classical – B if $S(B) \leq S(AB)$. The strange fact has been discovered: the decoherence may go faster by interaction of the environment with the classical subsystem. This has been called in Ref. [18] anomalous entanglement decay. As a result a number of open questions about nontrivial behavior of the open systems have been set, among them on asymmetry in the transfer of quantum information with respect to its direction.

In Rev. [18] asymmetric states were considered:

$$\rho_{AB} = q|\Psi_1\rangle\langle\Psi_1| + (1-q)|\Psi_2\rangle\langle\Psi_2|; 0 < q < 1. \quad (83)$$

With normalized $|\Psi_1\rangle = a|00\rangle + \sqrt{1-a^2}|11\rangle$ and $|\Psi_2\rangle = a|10\rangle + \sqrt{1-a^2}|01\rangle$ with $0 < a < 1$. From Eq. (83) it is seen that mixedness depends on q only, while the concurrence – on q and a . The expanded Eq. (83) is:

$$\rho_{AB} = \begin{pmatrix} qa^2 & 0 & 0 & qa\sqrt{1-a^2} \\ 0 & (1-q)(1-a^2) & (1-q)a\sqrt{1-a^2} & 0 \\ 0 & (1-q)a\sqrt{1-a^2} & (1-q)a^2 & 0 \\ qa\sqrt{1-a^2} & 0 & 0 & q(1-a^2) \end{pmatrix}. \quad (83a)$$

Hence:

$$S(AB) = -q \log_2 q - (1-q) \log_2 (1-q), \quad (84)$$

$$S(A) = -(a^2 - 2qa^2 + q) \log_2 (a^2 - 2qa^2 + q) - (1-a^2 + 2qa^2 - q) \log_2 (1-a^2 + 2qa^2 - q), \quad (85)$$

$$S(B) = -a^2 \log_2 a^2 - (1-a^2) \log_2 (1-a^2), \quad (86)$$

$$i_{B|A} = \frac{S(AB) - S(A)}{S(B)}; i_{A|B} = \frac{S(AB) - S(B)}{S(A)} \quad (87)$$

$$C = 2\sqrt{a^2(1-a^2)} |1-2q|. \quad (88)$$

Always $S(A) \geq S(AB)$, $S(B)$ may be more as well as less than $S(AB)$. According to definition of Ref. [18] the subsystem A is almost always quantum, while the subsystem B may be either quantum or classical. In Fig. 13 the dependences of $i_{B|A}$, C and $\text{Tr}\rho_{AB}^2$ on q and a^2 which have the expected appearance. Only the dependence of $i_{B|A}$ on a^2 is nontrivial. That the $i_{B|A}$ is almost always negative (except of the case $q = \frac{1}{2}$) just reflects the fact that the subsystem A is almost always quantum. At the maximal mixedness, achieved at $q = \frac{1}{2}$, the subsystem are not entangled but classically maximally correlated ($i_{B|A} = 0$) at any a^2 .

The dependences of c_2 and γ on q and a^2 are presented in Fig.14. The positive value of c_2 shows that at almost all q and a^2 A is the cause and B is the effect. Causality disappears ($c_2 = \infty$) only at $q = 0$ or 1 (the pure states) and $a^2 = \frac{1}{2}$ (the symmetric states). The direction of causal connection $A \rightarrow B$ clears up a conclusion of Ref. [18] about bigger fragility to decoherence of the classical subsystem B . Certainly the runoff quantum information occurs mainly in the effect B .

The states correspond to the subspaces IQ and IIIQ (Fig. 2), accordingly, the classical measure of causality γ in Fig. 14 shows either mistakenly opposite direction of causal connection or loses its meaning where γ is negative. Classical causality is absent ($\gamma = 1$) at $a^2 = q$ and $a^2 = 1-q$. The negative values of γ (subspace IIIQ) correspond to the positive values of the independence function $i_{A|B}$ or in other words, to the classicness of subsystem B by the definition of Ref. [18]. But since $c_2 > 0$ is *always* positive we conclude that anomalous entanglement decay by Ref. [18] is not anomalous, because it is only a particular case of general and natural phenomenon of more quantum information runoff on the more dissipative subsystem.

A nontrivial quantitative conclusion (which is impossible to make simply from appearance of the states (83) or (83a)) is that maximal mixed states $q = \frac{1}{2}$ correspond to the one-valued function line (Fig. 1). At any a^2 here $\gamma = 0$ (Fig. 14), that corresponds to the utmost irreversible transition $A \Rightarrow B$. This one-valued dependence of B on A is achieved at zero concurrence (Fig. 13). Therewith c_2 has any positive value depending on a^2 . In other words, the

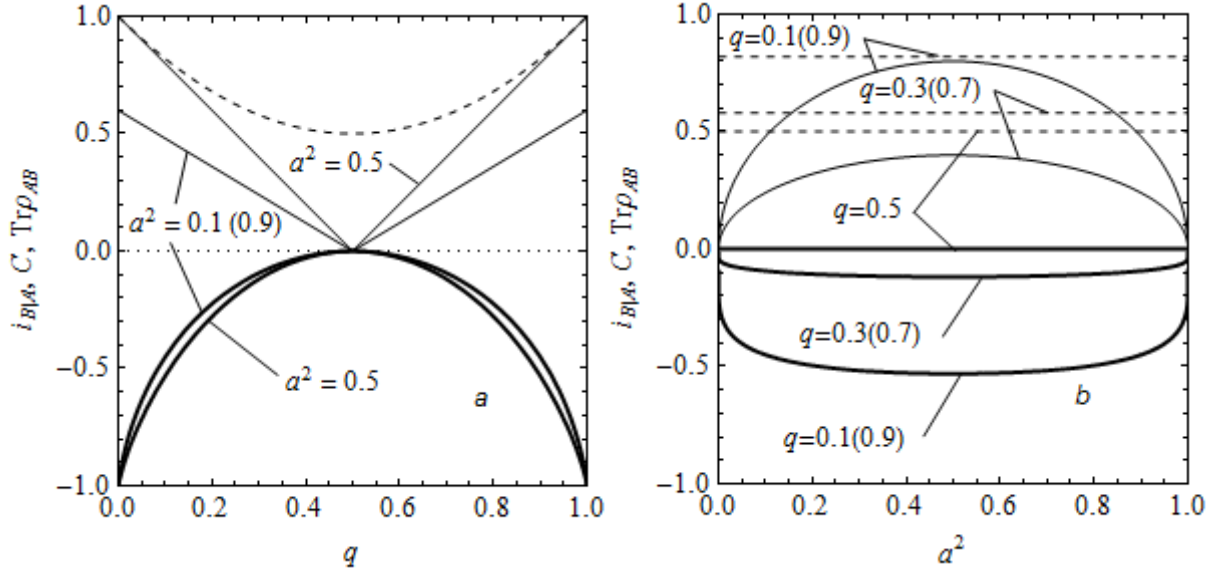


FIGURE 13. Dependence of $i_{B|A}$ (thick solid lines), C (fine solid lines), and $\text{Tr}\rho_{AB}^2$ (dashed lines) (a) on q and (b) on a^2 of the asymmetric “quantum-classical” states (83).

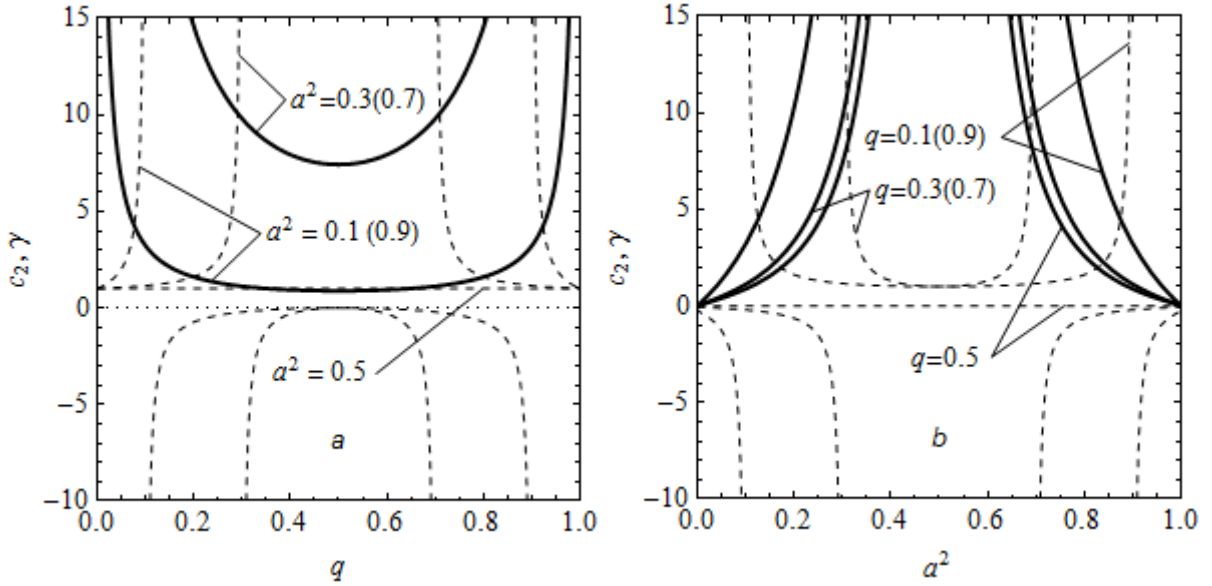


FIGURE 14. Dependence of c_2 (solid lines) and γ (dashed lines) (a) on q and (b) on a^2 of the asymmetric “quantum-classical” states (83).

case of the utmost strong classical causality can correspond to different degree of uniformly directed quantum causality – from the strongest one for the utmost asymmetry of the state ($a^2 \rightarrow 0$ or $a^2 \rightarrow 1$) to its absence at the symmetry ($a^2 = \frac{1}{2}$).

E. Thermal Entanglement under a Nonuniform External Magnetic Field

It is generally believed that increase of the temperature, as well as the magnetic field, destroy entanglement. But recently [40] it has been discovered that nonuniform magnetic field, on the contrary, play a constructive role and

entanglement is maintained at the high temperature as well as under the strong magnetic field. It has been found that just nonuniform magnetic field of opposite direction at the subsystem A and B has such decoherence suppression property.

Consider, according to Ref. [40], thermal entanglement of the two qubits with spin $\frac{1}{2}$ related by XY -Heisenberg interaction with the following Hamiltonian:

$$H = J(S_A^x S_B^x + S_A^y S_B^y) + B_A S_A^z + B_B S_B^z, \quad (89)$$

where the spin operator $S^j = \sigma^j / 2$ ($j = x, y, z$), J is the strength of Heisenberg interaction, B_A and B_B are the external magnetic fields at the particles A and B . The eigenvalues and eigenvectors of Hamiltonian (89) are:

$$H |00\rangle = -(B_A + B_B) |00\rangle, \quad (90)$$

$$H |11\rangle = (B_A + B_B) |11\rangle,$$

$$H |\Psi^\pm\rangle = \pm\sqrt{D} |\Psi^\pm\rangle,$$

where

$$|\Psi^\pm\rangle = \frac{1}{N_\pm} \left[|01\rangle + \frac{(B_A - B_B) \pm \sqrt{D}}{J} |10\rangle \right],$$

$$D = (B_A - B_B)^2 + J^2.$$

The density matrix of the thermal states is:

$$\rho_{AB} = \frac{1}{Z} \begin{pmatrix} e^{(B_A+B_B)/k_B T} & 0 & 0 & 0 \\ 0 & m+n & -s & 0 \\ 0 & -s & m-n & 0 \\ 0 & 0 & 0 & e^{-(B_A+B_B)/k_B T} \end{pmatrix}, \quad (91)$$

where

$$Z = \text{Tr} e^{-H/k_B T},$$

$$m = \text{ch}\left(\frac{\sqrt{D}}{k_B T}\right),$$

$$n = \frac{B_A - B_B}{\sqrt{D}} \text{sh}\left(\frac{\sqrt{D}}{k_B T}\right),$$

$$s = \frac{J \text{sh}\left(\frac{\sqrt{D}}{k_B T}\right)}{\sqrt{D}}.$$

In the next calculations we accept $k_B = J = 1$. The state asymmetry is determined by n .

From Eq. (91) follows:

$$S(AB) = -\frac{m+\sqrt{n^2+s^2}}{Z} \log_2 \frac{m+\sqrt{n^2+s^2}}{Z} - \frac{m-\sqrt{m^2+s^2}}{Z} \log_2 \frac{m-\sqrt{m^2+s^2}}{Z} - \frac{\exp(\frac{B_A+B_B}{T})}{Z} \log_2 \frac{\exp(\frac{B_A+B_B}{T})}{Z} - \frac{\exp(-\frac{B_A+B_B}{T})}{Z} \log_2 \frac{\exp(-\frac{B_A+B_B}{T})}{Z}, \quad (92)$$

$$S(A) = -\frac{\exp(\frac{B_A+B_B}{T})+m+n}{Z} \log_2 \frac{\exp(\frac{B_A+B_B}{T})+m+n}{Z} - \frac{\exp(-\frac{B_A+B_B}{T})+m-n}{Z} \log_2 \frac{\exp(-\frac{B_A+B_B}{T})+m-n}{Z}, \quad (93)$$

$$S(B) = -\frac{\exp(\frac{B_A+B_B}{T})+m-n}{Z} \log_2 \frac{\exp(\frac{B_A+B_B}{T})+m-n}{Z} - \frac{\exp(-\frac{B_A+B_B}{T})+m+n}{Z} \log_2 \frac{\exp(-\frac{B_A+B_B}{T})+m+n}{Z}. \quad (94)$$

The independence functions are determined by the general formulae (87). The concurrence is:

$$C = 2 \frac{s-1}{Z}. \quad (95)$$

For investigation of the nonuniform field impact, accept at the beginning $T = 1$, $B_A = 5$, $B_B = 5p$.

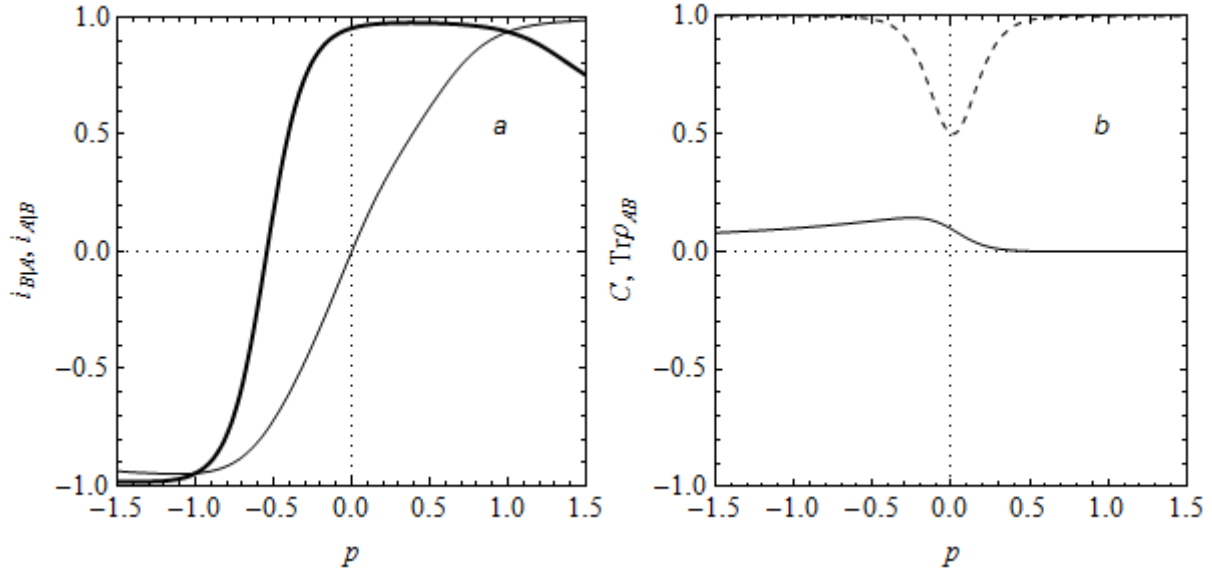


FIGURE 15. Dependence of (a) $i_{B|A}$ (thick solid line) and $i_{A|B}$ (fine solid line), (b) C (solid line) and $\text{Tr}\rho_{AB}^2$ (dashed line) on $p = B_B / B_A$ of the states (91) ($T = 1$).

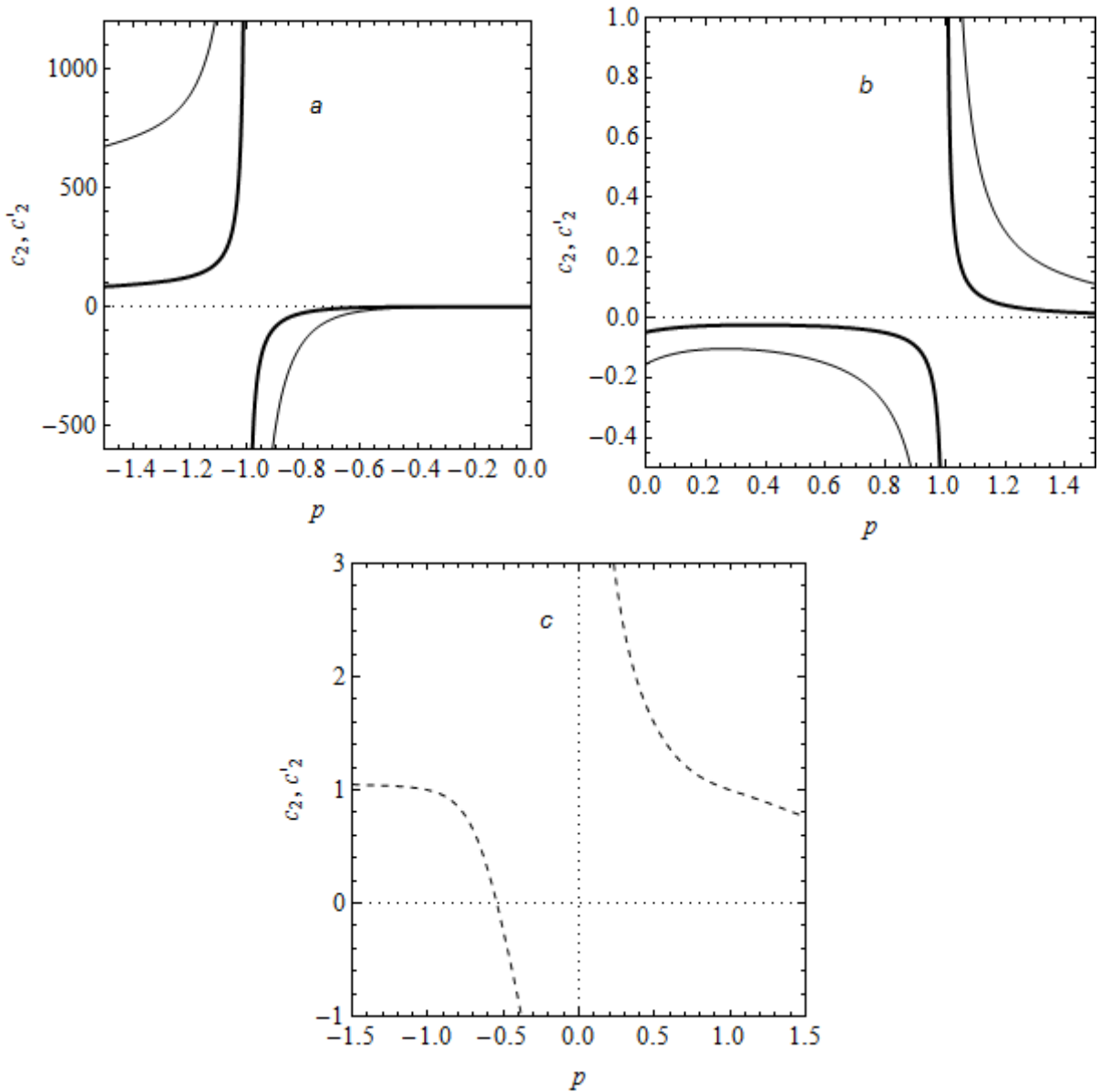


FIGURE 16. Dependence of (a, b) c_2 (thick solid line) and c'_2 (fine solid line), and (c) γ (dashed line) on $p = B_B / B_A$ of the states (91) ($T = 1$).

The maximal mixedness both by $\max S(AB)$ derived from Eq. (92), and by $\min \text{Tr} \rho_{AB}^2$ (Fig. 15) is achieved at $p \approx 0.010$. The concurrence in Fig. 15 demonstrates noted in Ref. [40] the most entanglement at oppositely directed fields at A and B , but the maximum is achieved not at the exact antisymmetry ($p = -1$) as presumed in Ref. [40], but at $p \approx -0.253$. Note, that according to Eqs. (93) and (94) $\max S(A)$ ($p \approx -0.149$) is close to $\max C$, while $\max S(B)$ is close to $\min \text{Tr} \rho_{AB}^2$ ($p \approx 0.08$), therewith $\max \alpha \approx 26.5$ is observed at $p \approx 0.176$. The independence function $i_{B|A}$ in Fig. 15 demonstrates similarity neither with the mixedness nor with the concurrence. $i_{B|A} \rightarrow -1$ that is quantum correlation increases at deeply negative p , where C decreases. At $-0.54 < p < 0.5$ $i_{B|A}$ is classically positive in spite of $C > 0$. $\max i_{B|A}$ that is the least correlation of the subsystem is observed at $p \approx 0.379$, where C is still finite. At big p $i_{B|A}$ goes down at the expense of classical correlations under the parallel fields. The independence function $i_{A|B}$ is also shown in Fig. 15. Although $i_{A|B} = 0$ at $p = 0$ there are no antisymmetry by p , $\min i_{A|B}$ is

observed at $p \approx -1.115$, while $i_{AB} \rightarrow 1$ at big positive p . In the interval $0 < p < 0.5$ the states are entangled though classically correlated (the both i are positive). Thus, the independence functions demonstrate nontrivial relation between quantum and classical correlations, which is impossible to reveal from consideration of the concurrence only.

Consider the causal connection of the subsystems. In this case determine c_2 not only at $k = \Delta r / \delta t = 1$ in Eq. (12), but drawing on the eigenvalues of Hamiltonian (90), compute δt according to Eq. (18). Supposing now $\Delta r = 1$, determine $c'_2 = c_2 / \delta t$. In Fig. 16 c_2 , c'_2 and γ are presented. The former two as convenience (to show their maxima) are presented at two different scales for the parallel and antiparallel fields. According to all the three measures causality is absent at $p = \pm 1$, that is under equal parallel and antiparallel fields at A and B . The interval $p(-\infty, -1)$ corresponds to the subspace IQ, $p(-1, 0.54]$ – IIQ, $p[-0.54, 0]$ – IVQ, $p(0, 1)$ – IIC, $p(1, \infty)$ – IC. According to both the quantum measures at $|p| > 1$ A is the cause, B is the effect, and inversely at $|p| < 1$. In other words, the effect is always in the region of stronger field. It can be understood as stabilizing polarization of the qubit in the strong field, as a result of which the qubit becomes in more degree the runoff of information than the source. At directionality of causal connection $A \rightarrow B$ and $|p| \rightarrow \infty$ causality is amplified: $c_2 \rightarrow +0$, $c'_2 \rightarrow +0$. But at directionality $B \rightarrow A$ $\min |c_2|$ and $\min |c'_2|$ are not at $p = 0$ as could be supposed intuitively, but at finite $p \approx 0.364$ for c_2 and $p \approx 0.266$ for c'_2 . These values of p are determined by the chosen temperature $T = 1$. Calculation shows that specific field ratio p at which causality is strongest decreases as the temperature increases. The causality function γ gives the right answer about directionality of causal connection only at $p > 0$. At last from Fig. 16 it is seen that there is no a qualitative difference between c_2 and c'_2 .

Consider the temperature influence more closely. It can be expected that any correlations decrease as the temperature increases. On the other hand, namely finite temperature leads to the mixing, which is a necessary condition of quantum causality. Indeed, as the temperature increases $S(AB)$ increases, however the subsystem entropies increases too, but by different manner, and one can expect nontrivial behavior of the entropic functions.

From Fig. 17 it is seen that mixedness increases with the temperature, but the magnetic field at the subsystem B suppresses this temperature influence. The concurrence (Fig. 18) under antiparallel fields, in accordance with the main conclusion of Ref. [40] is maintained at the high temperature. However the most suppression of decoherence is achieved not in the antisymmetric case ($p = -1$), but under stronger field at B ($p = -1.5$). At $T \rightarrow 0$, on the contrary, the highest concurrence is achieved under zero field at B . At positive p the concurrence steeply disappears in accordance with common view about suppression of entanglement by the magnetic field.

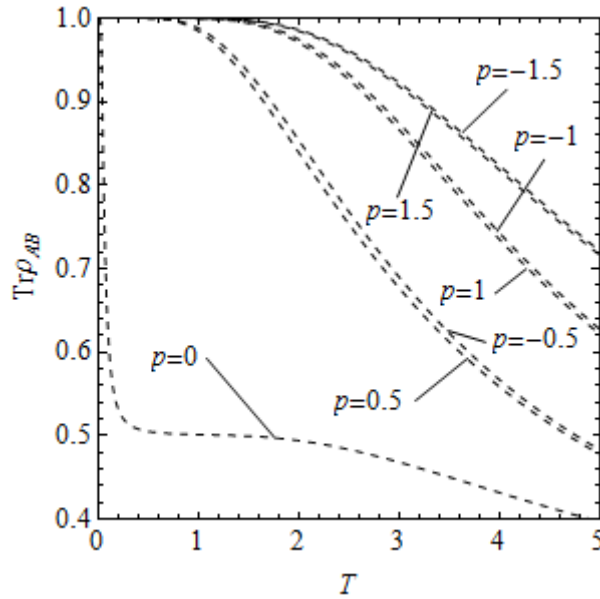


FIGURE 17. 17. Dependence of $\text{Tr} \rho_{AB}^2$ on T of the states (91).

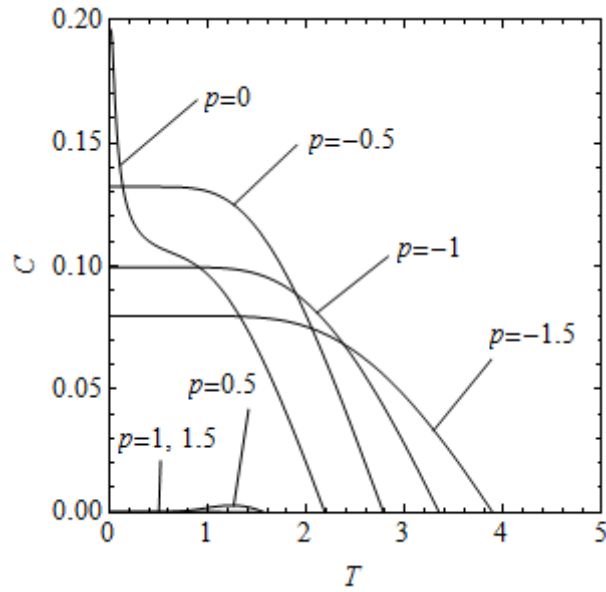


FIGURE 18. Dependence of C on T of the states (91).

The independence function $i_{B|A}$ (Fig. 19) points out monotonous amplification of quantum and classical correlations with amplification of negative field ratio p . At positive p correlations are classical and the temperature dependence is not monotonous – there is a minimum of positive $i_{B|A}$ (maximum of classical correlation) at the finite temperature. The inversed independence function $i_{A|B}$ (Fig. 20) has much smaller sensitivity of the temperature variation to the negative p , but much greater sensitivity to the positive p . At $p=0$ the curve $i_{A|B}(T)$ has the inflection point (at $T \approx 0.8$), which is absent in the curve $i_{B|A}$.

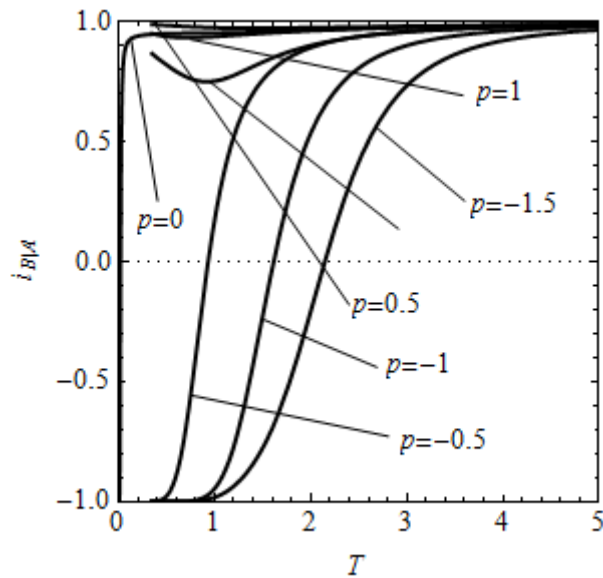


FIGURE 19. Dependence of $i_{B|A}$ on T of the states (91).

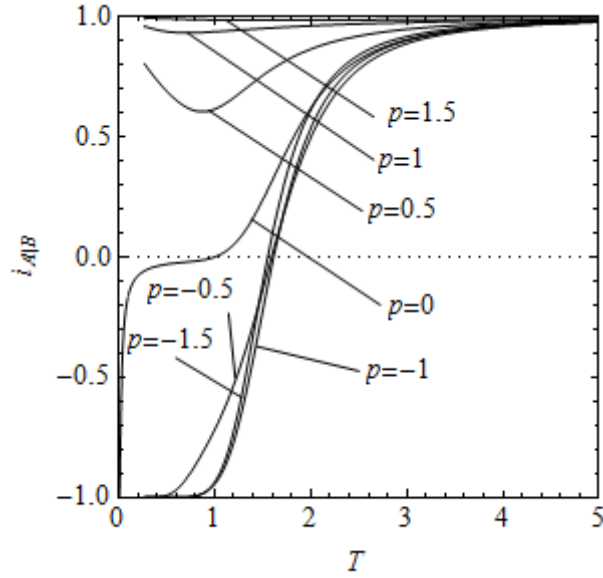


FIGURE 20. Dependence of $i_{A|B}$ on T of the states (91).

The classical measure of causality γ (Fig. 21) demonstrates that in the domain of its correct implementation ($p > 0$) directionality of causal connection is exactly independent of the temperature. There is only a weak amplification of the causal connection at $T \approx 0.9$. In the domain of its incorrect implementation ($p < 0$) γ demonstrates the breaks and causality reversals. In Fig 22 behavior of c_2 and c'_2 against the temperature is shown. At any p directionality of the causal connection is independent of the temperature, but its value depends on it. At $p > 0$, that is under the parallel fields, causality utmostly amplifies at the temperature tending to zero and remains almost steady at $T > 1.3$ (at $p = 0.5$ there is a very weak amplification of causality at the high temperature). Under the antiparallel fields ($p \leq 0$) causality, on the contrary considerably amplifies at the high temperature. The stronger field nonuniformity, the sharper this amplification. As it was accepted $J = 1$, $B_A = 5$ in the computations, hence it follows that Heisenberg interaction is essential for the causal connection only under the parallel fields.

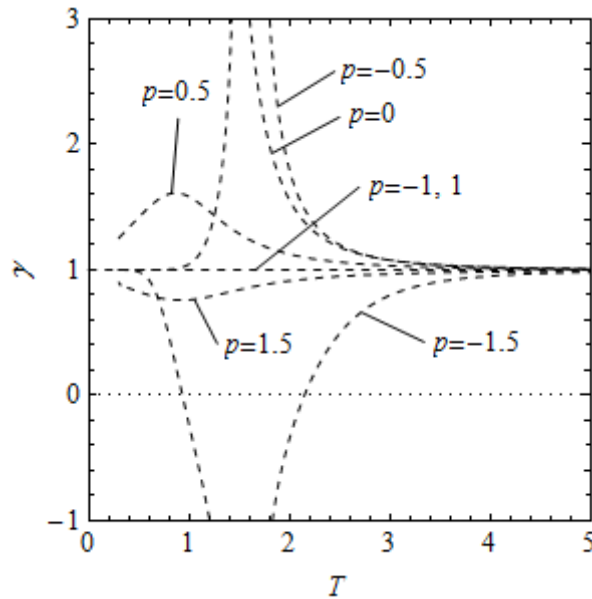


FIGURE 21. Dependence of γ on T of the states (91).

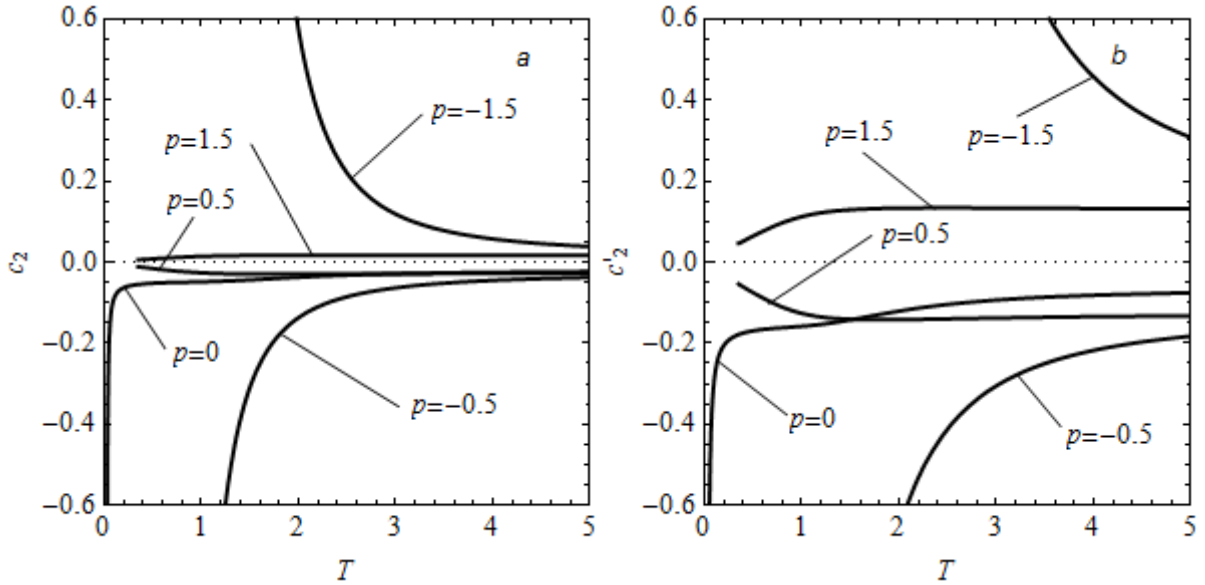


FIGURE 22. Dependence of (a) c_2 and (b) c'_2 on T of the states (91).

VI. CONCLUSION

The classical causal analysis had formalized the intuitive understanding of causality that, first, gave the possibility of its application to the complicated system analysis and, second, gave a quantitative measure of causality. The quantum extension of causal analysis has shown a richer picture of the subsystem causal connections, where the usual intuitive approach is hampered more commonly. The direction of causal connection is determined by the direction of irreversible information flow, and the quantitative measure of this connection c_2 is determined as the velocity of such flow. The absence of causality corresponds to $|c_2| \rightarrow \infty$, accordingly the degree of causal connection is inversely related to c_2 .

The independence functions used in the causal analysis allow classification of quantum and classical correlations of the subsystems, and their employment is of interest in any quantum systems, including those where causality is absent.

The possibilities of causal analysis have been demonstrated by the two series of examples of the two-partite two-state systems (qubits). The examples in both the series have been arranged in order from the simplest to the most nontrivial ones.

In the first series of the examples (Sec. IV) causality is absent; only the relationship between the independence function and the usual measures of entanglement and mixedness is revealed. It has been demonstrated that the independence function often but not always is determined by the state mixedness. Most important of all, in a number of cases the state can appear classical in entropic sense, but nevertheless be entangled.

In the second series of the examples (Sec. V) the systems with finite causality have been considered, beginning with the simplest example with asymmetric dissipation and ending with the enough complicated case of the qubits under a nonuniform external magnetic field at the different temperature. In every case the quantum measure of causality has been related with the classical one and it has been demonstrated that the latter often leads to apparent inversion of causal connection or meaninglessness. It has been shown the manner in which the distribution of entanglement in a three-partite system leads to the pairwise causal connection. For the case of asymmetric “quantum-classical” states the positive answer to the question, stated in Ref. [18] about availability of an asymmetry in the transfer of quantum information with respect to its direction, has been obtained. For the case of qubits under an external magnetic field the conclusions about nonuniformity field control of directionality of the causal connection have been obtained, which can be physically explained by the causal analysis results, but which could not be drawn without them. It has been demonstrated that directionality of causal connection is unaffected by temperature, but its value is affected by temperature oppositely under the parallel and antiparallel fields.

Application of the causal analysis to the systems with the number of states more than two should present no problems in itself, except the usual build-up of calculation cumbersomeness of the density matrix eigenvalues. A genera-

lization to multipartite system involves some complication of the mathematics, but since in the classical case it had successfully done before, one would hope that in the quantum case it should present no problems too.

REFERENCES

1. N. A. Kozyrev, "On the possibility of experimental investigation of the properties of time", in *Time in Science and Philosophy*, edited by J. Zeman, Prague: Academia, 1971, pp. 111-132.
2. S. M. Korotaev, *Galilean Electrodynamics* **4**, 86-90 (1993).
3. S. M. Korotaev, *Geomagnetism and Aeronomy* **32**(1), 27-33 (1992).
4. S. M. Korotaev, O. A. Hachay, and S. V. Shabelyansky, *Geomagnetism and Aeronomy* **32**(1), 48-53 (1992).
5. S. M. Korotaev, and O. A. Hachay, *Izvestia Phys. of the Solid Earth* **4**, 52-61 (1992).
6. S. M. Korotaev, O. A. Hachay, and L. K. Low, *Izvestia Phys. of the Solid Earth* **5**, 35-44 (1992).
7. S. M. Korotaev, S. V. Shabelyansky, and V. O. Serdyuk, *Izvestia Phys. of the Solid Earth* **6**, 77 (1992).
8. O. A. Hachay, S. M. Korotaev, and A. K. Troyanov, *Volcalonogy and Seismology* **3**, 92-100 (1992).
9. S. M. Korotaev, and O. A. Hachay, *Geomagnetism and Aeronomy* **32**(4), 119-121 (1992).
10. S. M. Korotaev, O. A. Hachay and S. V. Shabelyansky, *Geomagnetism and Aeronomy* **33**(2), 128-133 (1993).
11. M. L. Arushanov, and S. M. Korotaev, *Meteorology and Hydrology* **6**, 15-22 (1994).
12. S. M. Korotaev, *Geomagnetism and Aeronomy* **35**(3), 387-393 (1995).
13. S. M. Korotaev, V. O. Serdyuk, V. I. Nalivaiko, A. V. Novysh, S. P. Gaidash, Yu. V. Gorokhov, S. A. Pulinets and Kh. D. Kanonidi, *Phys. of Wave Phenomena* **11**, 46-55 (2003).
14. S. M. Korotaev, A. N. Morozov, V. O. Serdyuk, J. V. Gorohov and V. A. Machinin, *NeuroQuantology* **3**, 275-294 (2005).
15. S. M. Korotaev, *Int. J. of Computing Anticipatory Systems* **17**, 61-76 (2006).
16. S. M. Korotaev, V. O. Serdyuk and J. V. Gorohov, *Hadronic Journal* **30**, 39-56 (2007).
17. S. M. Korotaev and V. O. Serdyuk, *Int. J. of Computing Anticipatory Systems* **20**, 31-46 (2008).
18. K. Zyczkowski, P. Horodecki, M. Horodecki and R. Horodecki, *Phys. Rev. A* **65**, 012101 (2002).
19. C. E. Shannon and W. Weaver, *The Mathematical Theory of Communication*, Urbana: University of Illinois Press, 1949.
20. N. J. Cerf and C. Adami, *Phys. Rev. A* **60**, 893-897 (1999).
21. N. J. Cerf, *Phys. Rev. A* **57**, 3330-3347 (1998).
22. J. G. Cramer, *Phys. Rev. D* **22**, 362 (1980).
23. S. Mukohyama, *Phys. Rev. D* **58**, 104023 (1998).
24. A. Borras, A. R. Plastino, M. Casas and A. Plastino, *Phys. Rev. A* **78**, 052104 (2008).
25. W. K. Wootters, *Phys. Rev. Lett.* **80**, 2245-2248 (1998).
26. W. Dür, *Phys. Rev. A* **63**, 020303 (2001).
27. S. S. Jang, Y. W. Cheong, J. Kim and H. W. Lee, *Phys. Rev. A* **74**, 062112 (2006).
28. W. Song and Z.-B. Chen, *Phys. Rev. A* **76**, 014307 (2007).
29. M. B. Plenio, S. F. Huelga, A. Beige and P. L. Knight, *Phys. Rev. A* **59**, 2468-2475 (1999).
30. A. M. Basharov, *J. Exp. Theor. Phys.* **94**, 1070-1081 (2002).
31. M. B. Plenio and S. F. Huelga, *Phys. Rev. Lett.* **88**, 197901 (2002).
32. M. S. Kim, J. Lee, D. Ahn and P. L. Knight, *Phys. Rev. A* **65**, 040101 (2002).
33. D. Braun, *Phys. Rev. Lett.* **89**, 277901 (2002).
34. L. Jakobczyk, *J. Phys. A* **35**, 6383-6392 (2002).
35. F. Benatti, R. Floreanini and M. Piani, *Phys. Rev. Lett.* **91**, 070402 (2003).
36. T. Choi and H.J. Lee, *Phys. Rev. A* **76**, 012308 (2007).
37. W. J. Munro, D. F. V. James, A. G. White, and P. G. Kwiat, *Phys. Rev. A* **64**, 030302 (2001).
38. A. K. Rajagopal and R. W. Rendell, *Phys. Rev. A* **65**, 032328 (2002).
39. A. K. Rajagopal and R. W. Rendell, *Phys. Rev. A* **66**, 022104 (2002).
40. Y. Sun, Y. Chen and H. Chen, *Phys. Rev. A* **68**, 044301 (2003).